Computer Methods and Programs in Biomedicine 219 (2022) 106758

Contents lists available at ScienceDirect

Computer Methods and Programs in Biomedicine

journal homepage: www.elsevier.com/locate/cmpb

Spatial dynamics of dengue fever spreading for the coexistence of two serotypes with an application to the city of São Paulo, Brazil

F.M.M. Pereira, P.H.T. Schimit*

Informatics and Knowledge Management Graduate Program, Universidade Nove de Julho, Rua Vergueiro, 235/249 São Paulo, 01525-000, SP, Brazil

ARTICLE INFO

Article history:
Received 26 August 2021
Revised 8 February 2022
Accepted 12 March 2022

Keywords:
Basic reproduction number
Dengue
Probabilistic cellular automata
Spatial basic reproduction number
Spatial dynamics

ABSTRACT

Background and objective: Dengue fever is a disease in which individuals' spatial distribution and *Aedes aegypti* mosquitoes breeding places are important factors for the disease dynamics. Typically urban, dengue is a problem for least developed countries due to the ineffectiveness in controlling the vector and disorderly urbanization processes. The result is a composition of urban sanitation problems and areas with high demographic densities and intense flows of people. This paper explores the spatial distribution of vector breeding places to evaluate introducing a new dengue serotype to a population at equilibrium for a pre-existing serotype. The paper's objective is to analyze the spatial dynamics of dengue using variations of the basic reproduction number.

Methods: A model based on probabilistic cellular automata is proposed to permitting the necessary flexibility to consider some spatial distributions of vector breeding places. Then, ordinary differential equations are used as a mean-field approach of the model, and the basic reproduction number (R_0) is derived considering the next-generation matrix method. A spatial approach for R_0 is also proposed, and the model is tested in a neighbourhood from the city of São Paulo, Brazil, to examine the potential risks of vector breeding cells distribution.

Results: The results indicated that the more spread out these places, the higher are the values of R_0. When the model is applied to a neighbourhood in São Paulo, residential areas may boost the infections and must be under public vigilance to combat vector breeding sites.

Conclusions: Considering the mean-field approximation of the cellular automata model by ordinary differential equations, the basic reproduction number derived returned an estimative of the disease dynamics in the population. However, the spatial basic reproduction number was more assertive in showing areas with a higher disease incidence. Moreover, the model could be easily adapted to be used in real maps enabling simulations closer to real problems.

1. Introduction

Dengue is responsible for 96 million symptomatic cases and an estimated 40,000 death per year globally; also, around 3.9 billion people in 129 countries lives in risk regions for dengue [6,44,46]. Despite the efforts to combat and control the disease, dengue is one of the oldest diseases that humankind has contact [6,26,45,53].

Having the vector for transmitting the disease as the *Aedes aegypti* female mosquito, the dengue fever has a peculiar problem: sequential infections may evolve to dengue shock syndrome, increasing disease severity due to a process called *antibody-dependent enhancement* [12,21,22,40]. This is a big concern for a disease with five antigenically distinct viruses: DENV-1, DENV-2, DENV-3, DENV-4 and DENV-5 [1,20], given that an individual has life-long immunity to the cured case serotype and a temporary low cross-immunity of 3 to 9 months for other serotypes [1,32,47,61]. In Brazil, there is a concern that the co-circulation of multiple dengue serotypes, called *hyperendemicity*, is becoming standard for an increasing number of cities and metropolitan regions [11,17,59]. This is a problem since the 1990 decade, and it was confirmed by a few studies which report the presence of individuals with antibodies to three serotypes in northeastern Brazil in 2005 [4,8,24,41], and the four serotypes with simultaneous circulation in Manaus [3,4,50].

The *Aedes aegypti* females mosquitoes breed in clean still water and go in search of human blood, reaching distances of eight hundred meters in six days [27]. Therefore, it is a disease with

* Corresponding author.
E-mail addresses: fernandamoran@uninove.edu.br (F.M.M. Pereira), schimit@alumni.usp.br, schimit@uni9.pro.br (P.H.T. Schimit).

https://doi.org/10.1016/j.cmpb.2022.106758
0169-2607/

spreading dynamics dependent on the spatial distribution of humans, vectors and places of standing water. For instance, the work reported in Freitas et al. [18] showed that cases of dengue, zika and chikungunya were not detected at the same location and time in Rio de Janeiro in 2015/2016, with the reasons raised by the authors related to the spatial dynamics of the diseases: competition between viruses for breeding resources, and change in behaviour of susceptible human population as a response to increasing cases in the area. Such cases clusters were also studied in Bhoomiboonchoo et al. [5], where the depletion of cases occurred after spatial and temporal targeted interventions. Finally, other studies considered the landscape and seasonality to describe and predict dengue cases [31,49,62].

Therefore, the objective of this paper is to explore the spatial distributions of breeding places for mosquitoes in a model based on probabilistic cellular automata [47] for the co-circulation of two strains of the dengue virus. The basic reproduction number (R_0) is derived from the ordinary differential equations (ODE) proposed as a mean-field approximation of the cellular automata. Moreover, we propose a method for estimating the spatial basic reproduction number (R_0^S) to understand the real impact of this spatial configuration on the disease outbreak. The following points summarize the novelty of the paper: consider two dengue serotypes for numerical spatial analysis, given that many regions in Brazil face such a problem [3,11,59]; explore spatial distributions of mosquitoes breeding places; obtain the basic reproduction number for a model which takes into account the severity of a second infection of dengue; propose a spatial numerical basic reproduction number based on similar processes of spatial analysis; use the model for an accurate population distribution to estimate the impact of mosquitoes breeding places in residences and public spaces.

The basic reproduction number is "an epidemiologic metric used to describe the contagiousness or transmissibility of infectious agents" [13]. It represents the number of secondary infections from a single infected individual in a population fully susceptible to the disease. When ordinary differential equations (ODE) are used for compartmental models, R_0 is also a bifurcation parameter, where its value comes from the stability analysis of the system [28,33].

Regarding vector-borne diseases, R_0 can be interpreted as the number of secondary disease cases in humans from a single infected human individual in a population of humans and vectors completely susceptible [7]; which is a metric most often used due to the difficulty of estimating biological and environmental mosquitoes information [13,28,38,43,58]. The value of R_0 for dengue depends on many variables, such as population density, social organization, and weather seasonality [13], with global warming being a concern as it may increase the R_0 of dengue in temperate regions [34].

The next-generation matrix can be used to derive the basic reproduction number. The matrix is formed by the infectious subsystem of a compartmental model linearised about the disease-free equilibrium state. It represents the expected number of secondary infections caused by a single infected individual for a population entirely susceptible for each combination of row and columns of the matrix. This method was first described in Diekmann et al. [15] and further elaborated in Van Den Driessche and Watmough [56]. Here, the basic reproduction number is calculated from the ordinary differential equations using the next-generation matrix [60]. The ODE parameters are obtained from the probabilistic cellular automata simulations, in which multiple breeding places distributions are used.

Heterogeneous spatial distributions of human and vector populations require alternatives for modelling vector-borne diseases dynamics. Releases of female *Aedes aegypti* and *Aedes albopictus* to estimate their flight range is an example of an experimental process to evaluate the spatial infection spreading in Rio de Janeiro, Brazil [27]. In the same city, patches of the map representing neighbourhoods were used to detect spatio-temporal clustering of dengue, chikungunya and Zika, assessing the cases of the disease per patch [18]. Patches of maps have also been used for space-time scan statistical analyses of dengue in China [62], and to mapping the basic reproduction number for vector-borne diseases in Netherlands [25]. Still, in the Hartemink et al. study, the basic reproduction number is calculated for 107 spots in the map, representing the local situation in these regions. Mathematical models demonstrate that the spatial density of the winged female *Aedes aegypti* and the aquatic form of mosquitoes are distance-dependent to breeding sites [5,16]. Therefore, studies consider the distance to a point in the map as a variable to determine epidemiological parameters, such as the basic reproduction number [39], mosquito eggs count in a map [49], and the probability of being bitten by a tick in forests [57].

A water supply crisis took place in the southeast Brazil region in 2014–2015. It was partly responsible for a peak in annual dengue cases since households started to store water in inappropriate compartments, which helped the multiplication of mosquito breeding sites. Only in the city of São Paulo, more than 100,000 cases have been reported in 2015 [55]. This is one of the reasons to apply the developed model and methodology for a neighbourhood in São Paulo. Two scenarios are tested to explore the dynamics of the spatial distributions of vector breeding sites. The first considers that these breeding sites are on residential areas, and the second considers public squares, parks and schools.

This paper is organized as follows: the next section contains the methodology and description of the models, the results of the simulations are in Section 3, and a final discussion is presented in Section 4.

2. Methods

The human population is based on a probabilistic cellular automaton with cells representing individuals in one of the disease's states. The lattice is square with side n and a total human population of $N_H = n \times n$, and the neighbourhood, i.e., the neighbour cells that individuals visit per time step consists of C visits inside a Moore radius r per time step. The neighbourhood is different at each time step, with the C visits being randomly chosen according to the following procedure: the individual has a probability of visiting a cell in layer i given by $q_{i,r} = 2(r+1-i)/r(r+1)$. By layer i, consider the cells that are at a Chebyshev distance of i. With the layer chosen, a random cell of that layer is considered [37,51,52].

The mosquito *Aedes aegypti* is the vector for dengue. In order to standardize the terminology, we will refer only as vector in the model. On the vector side, the population consisting of N_V individuals are generated on breeding cells moving to neighbour cells once per time step according to a similar rule of human cells visits. Therefore, at the end of the time step, the last command concerns the vector movements, where each vector moves to a cell inside a Moore radius $r/2$, using the same random process to choose the neighbour used in human cells visits. Note that we consider that vectors may move to a cell half the maximum distance of human visits.

When visiting a cell, a human individual can be bitten by vectors with a probability P_B. In this process, susceptible humans can become diseased by infected vectors, and susceptibles vectors can become infected by sick individuals. Therefore, when a human visits a cell, each vector has a probability of biting of P_B, which confers the infection for the human. By using this approach $S_{1,2}$ can become I_1 or I_2 if bitten by vectors I_{V1} or I_{V2}, respectively. Susceptible individuals of strain type 1 only (S_1), and strain type 2 only

(S_2) may also be infected when bitten, becoming $I_{1/2}$ (strain type 1 infection given that already had the strain type 2 infection) or $I_{2/1}$ (strain type 2 infection given that already had the strain type 1 infection). Vectors S_V can become infected by strain type 1 (I_{V1}) when biting I_1 or $I_{1/2}$ human individuals, and infected by strain type 2 (I_{V2}) when biting I_2 or $I_{2/1}$ (related to the process associated with probability P_B).

Once infected, individuals I_1 and I_2 can be cured with probability P_{c1}, becoming S_2 and S_1, respectively. They can also die due to disease with probability P_{d1}. For individuals $I_{1/2}$ and $I_{2/1}$ probabilities of cure and death are P_{c2} and P_{d2}, and when these individuals get cured, the next state is the recovered to the considered strains (R). Finnaly, S_1, S_2 and R individuals may die due to other causes with probability P_n. $S_{1,2}$-individuals replace the dead ones to keep the population constant. We consider that the sequence of infection is irrelevant, but a case of a second infection during the lifetime increases P_d and decreases P_c due to antibody-dependent enhancement [12,22], thus $P_{c1} > P_{c2}$ and $P_{d1} < P_{d2}$. For the infected vectors, V_{I1} and V_{I2} have a probability P_{dV} of dying.

Therefore, one time step can be summarized to:

- human individuals visit C cells, and for each cell visit and vectors in that cell, the probability of bite is checked, affecting susceptible humans and vectors;
- for those human susceptibles who did not get infected, the state transition of dying due to other causes is tested;
- for the infected humans, cure and death due to the disease are tested in this order;
- for recovered humans, the state transition of dying due to other causes is tested;
- for the infected vectors, the probability of dying is tested;
- for each dead vector in the lattice, a new vector is generated on a random breeding cell;
- vectors move to a random neighbour cell, according to the method described;
- the states are synchronously updated at the end of the time step.

Ordinary differential equations (ODE) can be an mean-field approach for the probabilistic cellular automata model if we consider that the population is homogeneously distributed over space and each individual can interact with any other in the lattice [52]. Also, we consider that the mixing of susceptible and infected human individuals can generate new infections through the mosquitoes bites. Such an approach makes more straightforward the process of using real data to the model (it is easier to estimate parameter only for humans than for humans and vectors), and it has been used in other models [10,20,29,35,56,63]. Therefore, the equations can be written as follows for humans (similar to the model presented in Aguiar et al. [1]):

$$\begin{cases} \frac{dS_{1,2}(t)}{dt} & = -a_1 S_{1,2}(t)(I_1(t)+I_{1/2}(t)) - a_2 S_{1,2}(t)(I_2(t)+I_{2/1}(t)) \\ & \quad +c_1 I_1(t) + c_2 I_2(t) + c_{12} I_{1/2}(t) + c_{21} I_{2/1}(t) \\ & \quad +e_{S1} S_1(t) + e_{S2} S_2(t) + e_R R(t) \\ \frac{dS_1(t)}{dt} & = -a_{12} S_1(t)(I_1(t)+I_{1/2}(t)) + b_2 I_2(t) - e_{S1} S_1(t) \\ \frac{dS_2(t)}{dt} & = -a_{21} S_2(t)(I_2(t)+I_{2/1}(t)) + b_1 I_1(t) - e_{S2} S_2(t) \\ \frac{dI_1(t)}{dt} & = a_1 S_{1,2}(t)(I_1(t)+I_{1/2}(t)) - (b_1+c_1) I_1(t) \\ \frac{dI_2(t)}{dt} & = a_2 S_{1,2}(t)(I_2(t)+I_{2/1}(t)) - (b_2+c_2) I_2(t) \\ \frac{dI_{1/2}(t)}{dt} & = a_{12} S_1(t)(I_1(t)+I_{1/2}(t)) - (b_{12}+c_{12}) I_{1/2}(t) \\ \frac{dI_{2/1}(t)}{dt} & = a_{21} S_2(t)(I_2(t)+I_{2/1}(t)) - (b_{21}+c_{21}) I_{2/1}(t) \\ \frac{dR(t)}{dt} & = b_{12} I_{1/2}(t) + b_{21} I_{2/1}(t) - e_R R(t) \end{cases} \quad (1)$$

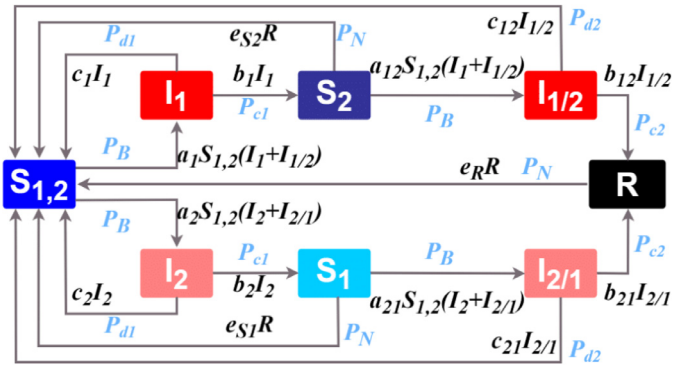

Fig. 1. The scheme of the dengue model for humans with two serotypes. Black letters are referred to ODE state transitions, and the blue letters to the associated probability in PCA model. (For interpretation of the references to colour in this figure legend, the reader is referred to the web version of this article.)

and as follows, for vectors

$$\begin{cases} \frac{dS_V(t)}{dt} & = -a_{V1} S_V(t) I_{V1}(t) - a_{V2} S_V(t) I_{V2}(t) \\ & \quad +c_{V1} I_{V1}(t) + c_{V2} I_{V2}(t) \\ \frac{dI_{V1}(t)}{dt} & = a_{V1} S_V(t) I_{V1}(t) - c_{V1} I_{V1}(t) \\ \frac{dI_{V2}(t)}{dt} & = a_{V2} S_V(t) I_{V2}(t) - c_{V2} I_{V2}(t), \end{cases} \quad (2)$$

where the rates are obtained from PCA simulations with a_1, a_2, a_{12} and a_{21} representing the infection constant rates for the transitions $S_{1,2} \to I_1$, $S_{1,2} \to I_2$, $S_1 \to I_{1/2}$, $S_2 \to I_{2/1}$, respectively; b_1, b_2, b_{12}, and b_{21} are the recovering constant rates for I_1, I_2, $I_{1/2}$, and $I_{2/1}$ individuals, respectively; c_1, c_2, c_{12}, and c_{21} are the death constant rates due to disease for I_1, I_2, $I_{1/2}$, and $I_{2/1}$ individuals, respectively; e_{S1}, e_{S2} and e_R are the constant rates for death due to other causes for S_1, S_2, and R individuals, respectively. For the vectors, a_{V1} and a_{V2} are the constant rates for the infection of S_V due to biting humans infected by strains 1 and 2, respectively; and c_{V1} and c_{V2} are the death constant rates for I_{V1} and I_{V2}. The scheme of the model for humans is shown in Fig. 1, where the black letters are referred to ODE state transitions, and the blue letters to the associated probability in PCA model.

Note that $dS_{1,2}(t)/dt + dS_1(t)/dt + dS_2(t)/dt + dI_1(t)/dt + dI_2(t)/dt + dI_{12}(t)/dt + dI_{21}(t)/dt + dR(t)/dt = 0$, and $dS_V(t)/dt + dI_{V1}(t)/dt + dI_{V2}(t)/dt = 0$, therefore the total number of human and vectors individuals is constant, with $S_{1,2}(t) + S_1(t) + S_2(t) + I_1(t) + I_2(t) + I_{12}(t) + I_{21}(t) + R(t) = N_H$, and $S_V(t) + I_{V1}(t) + I_{V2}(t) = N_V$. We assume that for the period analyzed, the number of deaths is equal to the number of births. The constant parameters from Eq. (4) can be obtained from PCA simulation using the expressions on Table 1.

Consider the expression $a_1 \approx \Delta I_1(t)_{S_{12} \to I_1} / (S_{12}(t)(I_1(t) + I_{1/2}(t))\Delta t$. It means the variation of I_1-individuals due to contamination of $S_{1,2}$-individuals per time step. The healing and death processes follow the same notation. The notation used in this manuscript is summarized in Table 2.

From the ODE, it is possible to derive the basic reproduction number (R_0) by using the Next-Generation Matrix (NGM), which is an alternative for models with finite categories of individuals [56]. From Eq. (1), the infectious subsystem is given by

$$\begin{cases} \frac{dI_1(t)}{dt} & = a_1 S_{1,2}(t)(I_1(t)+I_{1/2}(t)) - (b_1+c_1) I_1(t) \\ \frac{dI_2(t)}{dt} & = a_2 S_{1,2}(t)(I_2(t)+I_{2/1}(t)) - (b_2+c_2) I_2(t) \\ \frac{dI_{1/2}(t)}{dt} & = a_{1/2} S_1(t)(I_1(t)+I_{1/2}(t)) - (b_{12}+c_{12}) I_{1/2}(t) \\ \frac{dI_{2/1}(t)}{dt} & = a_{2/1} S_2(t)(I_2(t)+I_{2/1}(t)) - (b_{21}+c_{21}) I_{2/1}(t). \end{cases} \quad (3)$$

Table 1
Constant rates of the ODE model calculated from PCA simulation.

Contamination process (human)					
a_1	$\approx$	$\Delta I_1(t)_{S_{12}\to I_1}/(S_{12}(t)(I_1(t)+I_{1/2}(t))\Delta t$	a_2	$\approx$	$\Delta I_2(t)_{S_{12}\to I_2}/(S_{12}(t)(I_2(t)+I_{2/1}(t)))\Delta t$
a_{12}	$\approx$	$\Delta I_1(t)_{S_1\to I_{1/2}}/(S_1(t)(I_1(t)+I_{1/2}(t)))\Delta t$	a_{21}	$\approx$	$\Delta I_2(t)_{S_2\to I_{2/1}}/(S_2(t)(I_2(t)+I_{2/1}(t)))\Delta t$
Healing process (human)					
b_1	$\approx$	$\Delta S_2(t)_{I_1\to S_2}/I_1(t)\Delta t$	b_2	$\approx$	$\Delta S_1(t)_{I_2\to S_1}/I_2(t)\Delta t$
b_{12}	$\approx$	$\Delta R(t)_{I_{1/2}\to R}/I_{1/2}(t)\Delta t$	b_{21}	$\approx$	$\Delta R(t)_{I_{2/1}\to R}/I_{2/1}(t)\Delta t$
Death process due to disease (human)					
c_1	$\approx$	$\Delta S_{1,2}(t)_{I_1\to S_{1,2}}/I_1(t)\Delta t$	c_2	$\approx$	$\Delta S_{1,2}(t)_{I_2\to S_{1,2}}/I_2(t)\Delta t$
c_{12}	$\approx$	$\Delta S_{1,2}(t)_{I_{12}\to S_{1,2}}/I_{1/2}(t)\Delta t$	c_{21}	$\approx$	$\Delta S_{1,2}(t)_{I_{21}\to S_{1,2}}/I_{2/1}(t)\Delta t$
Death process due to other causes (human)					
e_{S1}	$\approx$	$\Delta S_{1,2}(t)_{S_1\to S_{1,2}}/S_1(t)\Delta t$	e_{S2}	$\approx$	$\Delta S_{1,2}(t)_{S_2\to S_{1,2}}/S_2(t)\Delta t$
e_R	$\approx$	$\Delta S_{1,2}(t)_{R\to S_{1,2}}/R(t)\Delta t$			
Contamination process (vector)					
a_{V1}	$\approx$	$\Delta I_{V1}(t)_{V_S\to I_{V1}}/(V_S(t)I_1(t))\Delta t$	a_{V2}	$\approx$	$\Delta I_{V2}(t)_{V_S\to I_{V2}}/(V_S(t)I_2(t))\Delta t$
Death process (vector)					
c_{V1}	$\approx$	$\Delta V_S(t)_{I_{V1}\to V_S}/I_{V1}(t)\Delta t$	c_{V2}	$\approx$	$\Delta V_S(t)_{I_{V2}\to V_S}/I_{V2}(t)\Delta t$

Table 2
Notation used in the paper.

Table of notation	
Notation	*Description*
N_H	Human population size.
N_V	Vector population size.
C	Number of visits to neighbours cells per individual per time step.
r	Maximum Moore radius for visits.
$S_{1,2}$	Human susceptible to strains 1 and 2.
S_1	Human recovered from strain 2, susceptible to strain 1 only.
S_2	Human recovered from strain 1, susceptible to strain 2 only.
I_1	Human infected by strain 1.
$I_{1/2}$	Human infected by strain 1, previously infected by strain 2.
I_2	Human infected by strain 2.
$I_{2/1}$	Human infected by strain 2, previously infected by strain 1.
R	Human recovered from strains 1 and 2.
S_V	Vector susceptible to strains 1 and 2.
I_{V1}	Vector infected by strain 1.
I_{V2}	Vector infected by strain 2.
P_B	Probability of bite.
P_{c1}	Probability of cure for a first infection by dengue in humans.
P_{c2}	Probability of cure for a second infection by dengue in humans.
P_{d1}	Probability of death for a first infection by dengue in humans.
P_{d2}	Probability of death for a second infection by dengue in humans.
P_n	Probability of death due to other causes in humans.
P_{dV}	Death probability of infected vectors.
a_1	Infection constant rate of $S_{1,2}$ individuals (becoming I_1).
a_{12}	Infection constant rate of S_1 individuals (becoming $I_{1/2}$).
a_2	Infection constant rate of $S_{1,2}$ individuals (becoming I_2).
a_{21}	Infection constant rate of S_2 individuals (becoming $I_{2/1}$).
b_1	Cure constant rate of I_1 individuals (becoming S_2).
b_{12}	Cure constant rate of $I_{1/2}$ individuals (becoming R).
b_2	Cure constant rate of I_2 individuals (becoming S_1).
b_{21}	Cure constant rate of $I_{2/1}$ individuals (becoming R).
c_1	Death constant rate of I_1 individuals due to disease.
c_{12}	Death constant rate of $I_{1/2}$ individuals due to disease.
c_2	Death constant rate of I_2 individuals due to disease.
c_{21}	Death constant rate of $I_{2/1}$ individuals due to disease.
e_{S2}	Death constant rate of S_2 individuals due to other causes.
e_R	Death constant rate of R individuals due to other causes.
a_{V1}	Infection constant rate of V_{S1} vector individuals (becoming I_{V1}).
a_{V1}	Infection constant rate of V_{S1} vector individuals (becoming I_{V2}).
c_{V1}	Death constant rate of I_{V1} vector individuals.
c_{V2}	Death constant rate of I_{V2} vector individuals.

For this subsystem, the Jacobian matrix is

$$J_{(I_1,I_2,I_{1/2},I_{2/1})} = \begin{bmatrix} a_1S_{1,2}-b_1-c_1 & 0 & a_1S_{1,2} & 0 \\ 0 & a_2S_{1,2}-b_2-c_2 & 0 & a_2S_{1,2} \\ a_{1/2}S_1 & 0 & a_{1/2}S_1-b_{12}-c_{12} & 0 \\ 0 & a_{2/1}S_2 & 0 & a_{2/1}S_2-b_{21}-c_{21} \end{bmatrix}$$

Then, the Jacobian matrix is decomposed as $T+\Sigma$, where T is the transmission part, containing the production of new infected, and Σ is the transition part, containing changes in the states [14], only for the infected states. With these matrices, we calculate the dominant eigenvalue (spectral radius) ρ of the matrix $-T\Sigma^{-1}$ at the disease-free equilibrium state $\left(S^*_{1,2}=1, S_1*=0, S_2*=0, I^*_1=0, I^*_{1/2}=0, I^*_2=0, I^*_{2/1}=0, R^*=0\right)$. Therefore:

$$T = \begin{bmatrix} a_1 & 0 & a_1 & 0 \\ 0 & a_2 & 0 & a_2 \\ 0 & 0 & 0 & 0 \\ 0 & 0 & 0 & 0 \end{bmatrix}$$

and

$$\Sigma = \begin{bmatrix} -(b_1+c_1) & 0 & 0 & 0 \\ 0 & -(b_2+c_2) & 0 & 0 \\ 0 & 0 & -(b_{12}+c_{12}) & 0 \\ 0 & 0 & 0 & -(b_{21}+c_{21}) \end{bmatrix}$$

The eigenvalues of $-T\Sigma^{-1}$ are: $R_{01}=\dfrac{a_1}{b_1+c_1}$ and $R_{02}=\dfrac{a_2}{b_2+c_2}$. Then, R_0 is given by

$$R_0 = \max\left(R_{01}, R_{02}\right). \tag{4}$$

This expression results from the ODE analysis, returning the bifurcation value of R_0, which changes the equilibrium state. In general, R_0 can be interpreted as the expected number of secondary cases, which can be approximated as the transmissibility times contact over time times the duration of the infection [13,30]. Note that this is exactly what Eq. (4) represents, where a_1 and a_2 are the transmissibility times contact over a time step rate, and $1/(b_1+c_1)$ and $1/(b_2+c_2)$ are the period, in time steps, of infectiousness.

Therefore, we propose a spatial approach for R_0, which will be denoted by R^S_0. Basically, for each cell with index (i,j) in the lattice, $R^S_0(i,j)$ is given by the Eq. (4), though considering the constant rates from Table 1 *only for the neighbourhood inside a Moore radius* r_{R_0}. This expression is given by:

$$R^S_0(i,j) = \max\left(\frac{a^S_1(i,j)}{b^S_1(i,j)+c^S_1(i,j)}, \frac{a^S_2(i,j)}{b^S_2(i,j)+c^S_2(i,j)}\right). \tag{5}$$

where:

$$
\begin{aligned}
a_1^S(i,j) &= \frac{\sum_{x=i-r_{R0}}^{x=i+r_{R0}} \sum_{y=j-r_{R0}}^{y=j+r_{R0}} \Delta I_1^S(x,y)_{S_{12}\to I_1}}{\sum_{x=i-r_{R0}}^{x=i+r_{R0}} \sum_{y=j-r_{R0}}^{y=j+r_{R0}} S_{12}^S(x,y) \sum_{x=i-r_{R0}}^{x=i+r_{R0}} \sum_{y=j-r_{R0}}^{y=j+r_{R0}} I_1^S(x,y) + I_{1/2}^S(x,y)} \\
b_1^S(i,j) &= \frac{\sum_{x=i-r_{R0}}^{x=i+r_{R0}} \sum_{y=j-r_{R0}}^{y=j+r_{R0}} \Delta S_2^S(x,y)_{I_1\to S_2}}{\sum_{x=i-r_{R0}}^{x=i+r_{R0}} \sum_{y=j-r_{R0}}^{y=j+r_{R0}} I_1^S(x,y)} \\
c_1^S(i,j) &= \frac{\sum_{x=i-r_{R0}}^{x=i+r_{R0}} \sum_{y=j-r_{R0}}^{y=j+r_{R0}} \Delta S_{1,2}^S(x,y)_{I_1\to S_{1,2}}}{\sum_{x=i-r_{R0}}^{x=i+r_{R0}} \sum_{y=j-r_{R0}}^{y=j+r_{R0}} I_1^S(x,y)} \\
a_2^S(i,j) &= \frac{\sum_{x=i-r_{R0}}^{x=i+r_{R0}} \sum_{y=j-r_{R0}}^{y=j+r_{R0}} \Delta I_1^S(x,y)_{S_{12}\to I_2}}{\sum_{x=i-r_{R0}}^{x=i+r_{R0}} \sum_{y=j-r_{R0}}^{y=j+r_{R0}} S_{12}^S(x,y) \sum_{x=i-r_{R0}}^{x=i+r_{R0}} \sum_{y=j-r_{R0}}^{y=j+r_{R0}} I_2^S(x,y) + I_{2/1}^S(x,y)} \\
b_2^S(i,j) &= \frac{\sum_{x=i-r_{R0}}^{x=i+r_{R0}} \sum_{y=j-r_{R0}}^{y=j+r_{R0}} \Delta S_1^S(x,y)_{I_2\to S_1}}{\sum_{x=i-r_{R0}}^{x=i+r_{R0}} \sum_{y=j-r_{R0}}^{y=j+r_{R0}} I_2^S(x,y)} \\
c_2^S(i,j) &= \frac{\sum_{x=i-r_{R0}}^{x=i+r_{R0}} \sum_{y=j-r_{R0}}^{y=j+r_{R0}} \Delta S_{1,2}^S(x,y)_{I_2\to S_{1,2}}}{\sum_{x=i-r_{R0}}^{x=i+r_{R0}} \sum_{y=j-r_{R0}}^{y=j+r_{R0}} I_2^S(x,y)}
\end{aligned}
\tag{6}
$$

where $S_1^S(x,y)$ is the number of S_1-individuals at position (x,y) of the lattice, and so on for the other states variables; and $\Delta I_1^S(x,y)_{S_{12}\to I_1}$ is the number of new infected I_1 individuals due to the contamination of S_{12}-individuals at position (x,y), and so on for the other deltas. Note that when r_{R_0} tends to the side of the lattice, i.e., $r_{R_0} \to n$ (recall that the lattice is a square with dimension $n \times n$), $a_1^S(i,j) \to a_1$, $b_1^S(i,j) \to b_1$, $c_1^S(i,j) \to c_1$, $a_2^S(i,j) \to a_2$, $b_2^S(i,j) \to b_2$, $c_2^S(i,j) \to c_2$, and consequently $R_0^S(i,j) \to R_0$, $\forall\, i,j$.

This is a numerical approach which considers that the R_0 in an area is obtained by using the local data. In [39], the authors introduced a new method for quantifying spatially adjusted R_0 with the objective of refecting spatial heterogeneity in transmission among individuals. The method proposed here is a numerical approach of their method since we take the average number locally for every point of the lattice. It is also a similar procedure applied in Hartemink et al. [25] which considered local properties in the map to calculate R_0 for vector-borne diseases.

In the next section, the results are presented.

3. Results

For the simulations, we consider a lattice with side $n = 200$, and $N_H = 200 \times 200 = 40,000$ human individuals. The vector constant population consists of $N_V = 72,000$ vector individuals initially distributed over the 3600 breeding cells. Further details will be explained later. The parameters for PCA simulations are $P_{c1} = 0.7$, $P_{d1} = 0.3$, $P_{c2} = 0.5$, $P_{d2} = 0.4$, $P_{dV} = 0.2$, and $P_B = 0.1$. The simulation runs for $t_s = 200$ time steps starting with the initial conditions $S_{1,2}(0) = 0.99$, $I_1(0) = 0.01$, and $I_2(0) = I_{1/2}(0) = I_{2/1}(0) = R(0) = 0$ for humans, and $S_V(0) = 0.99$, $I_{V1}(0) = 0.01$, and $I_{V2} = 0$ for vector. In order to consider the effect of a new dengue strain starting a new outbreak on a steady state situation of the population, we consider that at time step $t_s/2 = 100$, a quantity of $I_2(100) = 0.01$ human and $I_{V2}(100) = 0.01$ vector individuals replace the same quantity of $S_1, 2(100)$ and $S_V(100)$, respectively. Human individuals are homogeneously distributed over the lattice, and vector individuals are randomly placed only on vector breeding places as the initial condition. Finally, the movements characteristics are $C = 8$ and $r = 16$. These values were based on the study [47], with other combinations being tested obtaining dynamically similar results. Parameters are fixed for the study unless otherwise stated.

The spatial distribution of breeding places for vectors is a relevant feature for analyzing the propagation dynamic of dengue. We consider that some cells in the lattice are breeding places, meaning that only on these cells that vectors are generated, and only on these cells vector individuals are placed as the initial condition for the simulation (and also the distribution of new strain infected on the middle of the simulation). We consider five breeding cells distributions with 3600 cells and 20 vectors per cell on average, but the vector population is constant $N_V = 72,000$. The first distribution consists of a square with side 60 centred on the lattice. Following distributions have the lattice divided into 4, 9, 16 and 25 equal parts with centred squares of sides 30, 20, 15 and 12 cells on each part. Fig. 2 contains the five distributions, named β_1, β_4, β_9, β_{16} and β_{25}.

The first result to be presented is a comparison between PCA and ODE models. The ODE parameters are calculated from the PCA average results of the last 10 time steps by using equations from Table 1, and then applied to Eq. (4) (using a_1, a_{12}, a_2, a_{21}, b_1, b_{12}, b_2, b_{21}, c_1, c_{12}, c_2, c_{21}, e_{S2}, e_R) and 2 (using a_{V1}, a_{V1}, c_{V1}, c_{V2}). The ODE is numerically solved using the 4^{th}-order Runge-Kutta method with integration time step of 0.01. The initial conditions for ODE are $S_{1,2}(0) = 0.98$, $I_1(0) = I_2(0) = 0.01$, $I_{1/2}(0) = I_{2/1}(0) = R(0) = 0$ $S_V(0) = 0.98$, and $I_{V1}(0) = I_{V2} = 0.01$. Figs. 3 and 4 show the temporal evolution of PCA and ODE simulations, using breeding cells distributions β_4 and β_{25} in PCA. Note the good agreement between the two approaches when we compare the steady states of the simulation (where the ODE parameters are based on PCA simulation). It is worth noting that ODE is a mean-field approach for PCA, and this is the reason for a distinct initial transient along with the permanent regime data of PCA being used to simulate the ODE.

There is a difference in the levels of human and vector infected individuals according to the distribution simulated. Fig. 5 contains the normalized human and vector individuals concentrations when the system achieved the permanent regime for the five distributions considered. The number of infected humans increases and reaches a maximum value as the breeding sites are more spread in the lattice, and the opposite is true for infected vectors. Note that distribution β_1 concentrates vectors in a portion of the lattice as the humans are homogeneously distributed, causing the cycle of infections to be concentrated in this portion, exposing more the vectors than the humans. For the distribution β_{25}, humans and vectors are more equally distributed, which increases (decreases) the number of humans (vectors) infected in the lattice. This result demonstrates that the situation of the disease on the lattice cannot be analyzed by only using the number of infected individuals. The basic reproduction number is affected by space-time environmental conditions and the behaviour of the infected population. Therefore, it summarizes the moment of the disease in space and time.

In order to understand the influence of the bite probability, 1000 simulations are run considering P_B in the range $P_B = 0.001, 0.002, \ldots, 0.1$ to see how P_B influences R_0 when the system

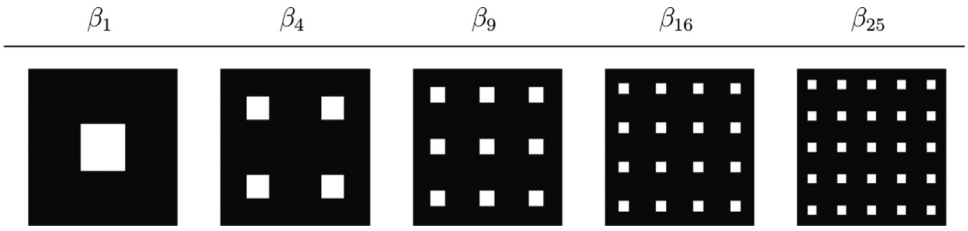

Fig. 2. Vector breeding cells in white for distributions β_1, β_4, β_9, β_{16} and β_{25}.

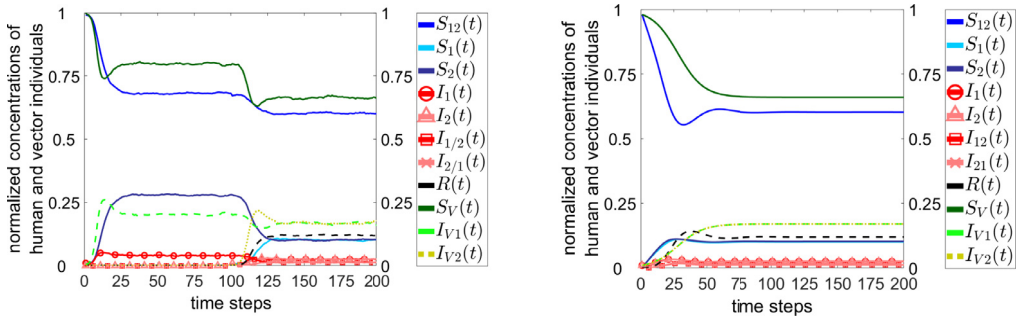

(a) PCA. (b) ODE.

Fig. 3. PCA and ODE simulations for distribution β_4.

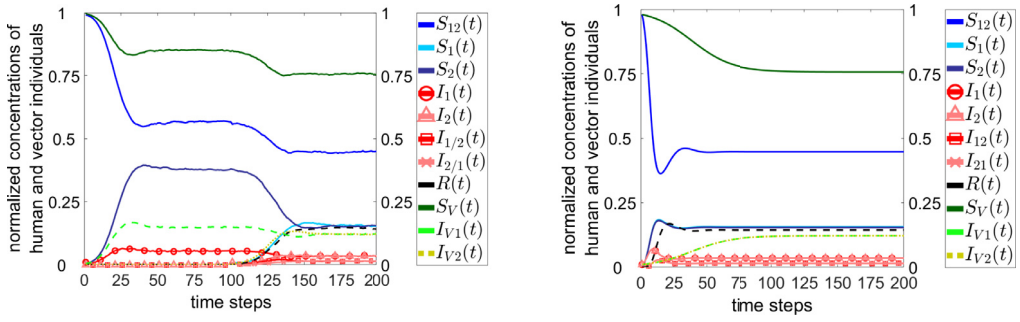

(a) PCA. (b) ODE.

Fig. 4. PCA and ODE simulations for distribution β_{25}.

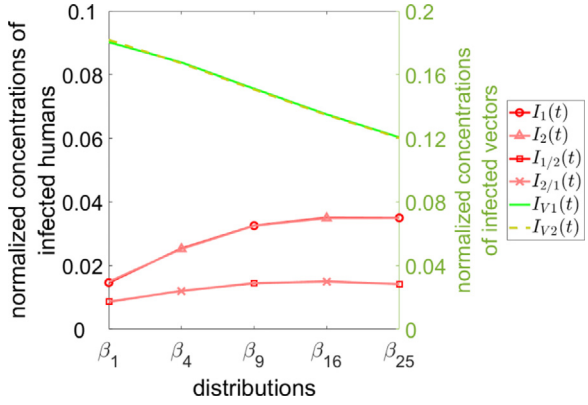

Fig. 5. Normalized human and vector individuals concentrations when the system achieved the permanent regime for the five distributions considered.

achieves the permanent regime. For each simulation, the average value of R_0 in the last 10 time steps is considered. Fig. 6 shows the results for the five vector breeding cells distributions for the first (Fig. 6a) and second (Fig. 6b) halves of the simulation. The more spread are the breeding cells in the lattice, the higher the basic reproduction number and higher is the increase in R_0 for an equal variation in P_B. Note that for the second half of the simulation, the value of R_0 has a slight decrease for all distributions. Since both strains are present and share the human population to infect individuals, we have $R_{01} \approx R_{02}$ (confirmed by raw data). From Eq. (4), the final value of R_0 is the maximum value between R_{01} and R_{02}. Therefore, both disease strains have the capacity to infect reduced due to this competition, and this reflects on the final R_0.

Using Eqs. (5) and (6), the spatial basic reproduction number $(R_0^S(i,j))$ for each cell of the lattice considering $r_{R_0} = 5$. Fig. 7 contains the maps of R_0^S for five distributions and time steps $t = 0$, $t = 5$, $t = 10$, $t = 20$, and $t = 30$. For these simulations, there is one strain present in the population, and a light colour represents a higher R_0^S, and the black colour represents $R_0^S(i,j) = 0$. Note that the lighter colours occur on distribution β_1, and from time step $t = 10$, the disease is present all over the lattice, except for β_1, and β_4.

Considering the standard deviation of R_0^S for the whole lattice as a measure of how distributed is R_0^S in the lattice, Fig. 8 has the time evolution of $\sigma_{R_0^S}(t)$ for the five distributions using $P_B = 0.1$. Therefore, distributions with larger vector breeding cells tend to have a disproportionate dispersion of cases in the population,

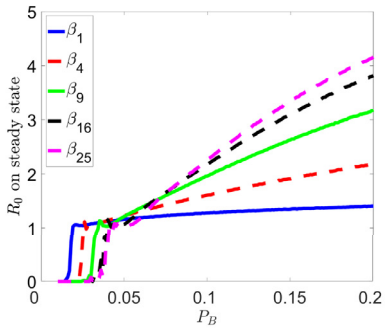

(a) R_0 for the system in steady state for the first half of the simulation.

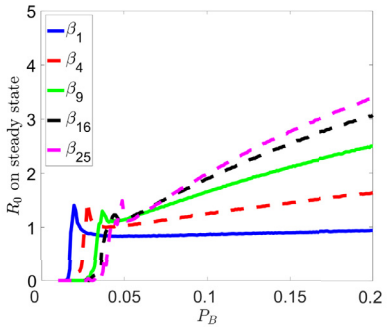

(b) R_0 for the system in steady state for the second half of the simulation, when the second strain is introduced.

Fig. 6. R_0 for the system in steady state for the first and second halves of the simulation. R_0 is calculated using data from the last 10 time steps of each half. Recall that the second half is featured by the introduction of a different dengue strain.

highlighting the importance of spatial dynamics in studying mosquitoes-borne diseases.

4. The model in a real map

The model is adapted to a real map for evaluating the impact of breeding cells over space. Therefore, we used a region from the east part of the São Paulo city called Vila Curuça, where there are some required characteristics on the map, such as residential neighbourhood, approximately 10,000 residents per square kilometre, and public areas consisting of squares, parks and children's education schools. Therefore, the map and the layers for each feature of the map were downloaded from [42] using the software QGIS [48]. The original map and the map to be used in simulations are in Fig. 9. Buildings in this region were considered as residential places, and public parks, squares and schools were considered public places. Points of no interest for the simulation were considered a mask.

We had to adapt the model for using it on the map due to the heterogeneous distribution of individual in residential areas. Consequently, each residential cell may have one or more individuals living in that space, what can represent a family. The total population is constant with $N_H = 10,000$, and the vector population varies according to the scenario considered, always with an averave number of 20 vectors per breeding cell. The initial condition for the simulations on the real map is based on a random distribution of susceptible individuals over the lattice with the possibility of one or more per residential cell. The rest of the configuration is similar to the simulations of the previous section ($t_s = 200$, $S_{1,2}(0) = 0.99$, $I_1(0) = 0.01$, and $I_2(0) = I_{1/2}(0) = I_{2/1}(0) = R(0) = 0$ for humans, and $S_V(0) = 0.99$, $I_{V1}(0) = 0.01$, and $I_{V2} = 0$ for vector; also for the new dengue strain, $I_2(100) = 0.01$ and $I_{V2}(100) = 0.01$). The movement is also set with $C = 8$ and $r = 16$. Considering the vector breeding cells distributions, we consider two scenarios:

- Scenario γ: A fraction f of public cells is considered to have a vetor breeding site;
- Scenario δ: A fraction f of residential cells is considered to have a vetor breeding site.

For each scenario, a fraction f of the cells identified as public or residential cells is considered as a vector breeding site. Fig. 10 contains the distribution of R_0^S at time step $t = 150$ (system in permanent regime with the co-existence of two serotypes) for both distributions and $f = 0.02, 0.04, 0.06, 0.08, 0.1$, using $P_B = 0.1$. Of course, the number of public cells is lower than residential; however, using the data available in Fig. 11, it is possible to conclude that residential cells are more relevant for increasing and reducing the incidence of cases over the lattice since the cells are more evenly spread over the lattice. Fig. 11 contains the average value of R_0 for the last 20 time steps when system achieved the permanent regime for different value of P_B and five values of f, for γ and δ cases.

5. Discussion

This paper proposed a model based on probabilistic cellular automata to study the dengue fever dynamics on a few spatial distributions of breeding places. Ordinary differential equations were used to derive the basic reproduction number from the next-generation matrix method. Simulations were set so that the population was in the steady state for one strain of the disease when another strain was added to the population. Five spatial distributions of breeding places were tested, and the cases with more spread vector breeding cells were responsible for higher values of the basic reproduction number.

Adapting the model for a real map was important for some reasons. The first is to show the flexibility of using the model in a real scenario. Thus, after separating the required information on the map, it is a direct to process to distribute individuals and vector breeding cells over the lattice. The same process can be used if more information about breeding sites is gathered. It is a powerful tool for estimating the impact of breeding sites on residences, a well known problem in Brazil, where even the residential waste is related to dengue cases [54]. Despite the lower number of public cells (and consequently of the portion of breeding cells), the disease can still be endemic in a region if the authorities do not inspect public places properly.

It is worth mentioning that this model type also helps to simulating a variety of cases when epidemiological parameters of the disease are laborious to estimate. For dengue, the number of female mosquitoes on residences during the peak cases in different countries varies from 1 to 20 [23]. Also, human to mosquito transmission rate is hard to estimate [36]. Here, these variables can be evaluated through testing different values of the bite probability (P_B), which has a direct influence over the constant rates a_1 and a_2 from ODE and used on R_0 and R_0^S. Finally, the variables related to infetiousness period for humans, and fatality rate for the first and second incidences of dengue for an individual (P_{C1}, P_{C2}, P_{D1}, P_{D2})

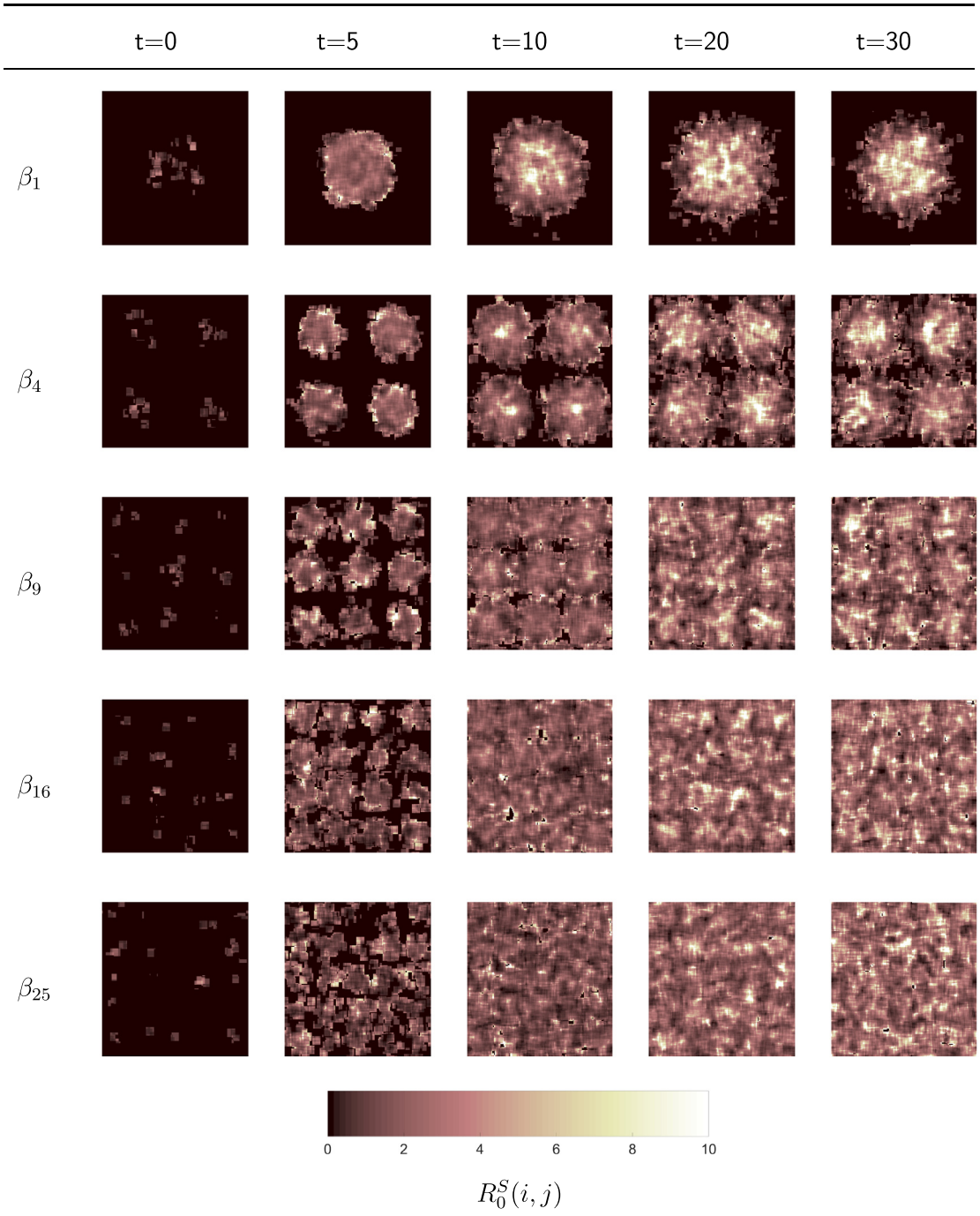

Fig. 7. Maps for the spatial basic reproduction number (R_0^S) for five distributions and five different time steps. Light colour represents a higher $R_0^S(i, j)$, and the black colour represents $R_0^S(i, j) = 0$.

have an influence over constant rates b_1, b_2, c_1, and c_2. The values used in simulation may not represent real values of the disease, though different values were tested with similar results in terms of dynamics, i.e., refining the use of the model can provide more precise results with the same dynamical profile.

Regarding the simulation results, there was a good agreement between PCA and ODE approaches, as presented in Figs. 3 and 4. These figures also show the time evolution of the human and vector states concentration on the lattice. The dynamics of the states transitions in the two populations is different because, unlike humans, vectors are not susceptible to suffering from a second infection since they have a relatively much shorter lifespan. From Fig. 5, note that the more spread are the vector breeding places, the lower is the number of infected vectors in the lattice; that is, the spreading of vectors is a critical factor for the disease R_0 (Figs. 6 and 7). Fig. 8 also shows that concentrated portions of the map with vector breeding cells are responsible for lower values of R_0, and a disproportionate dispersion of cases in the population. For more equally distributed vector breeding cells, a higher value of R_0 is less disproportionate over the lattice.

The results must also be analyzed regarding the second virus strain insertion in the population. This was possible due to the PCA model ability to track all variations in the number of individuals in different states. Therefore, the results indicate competition

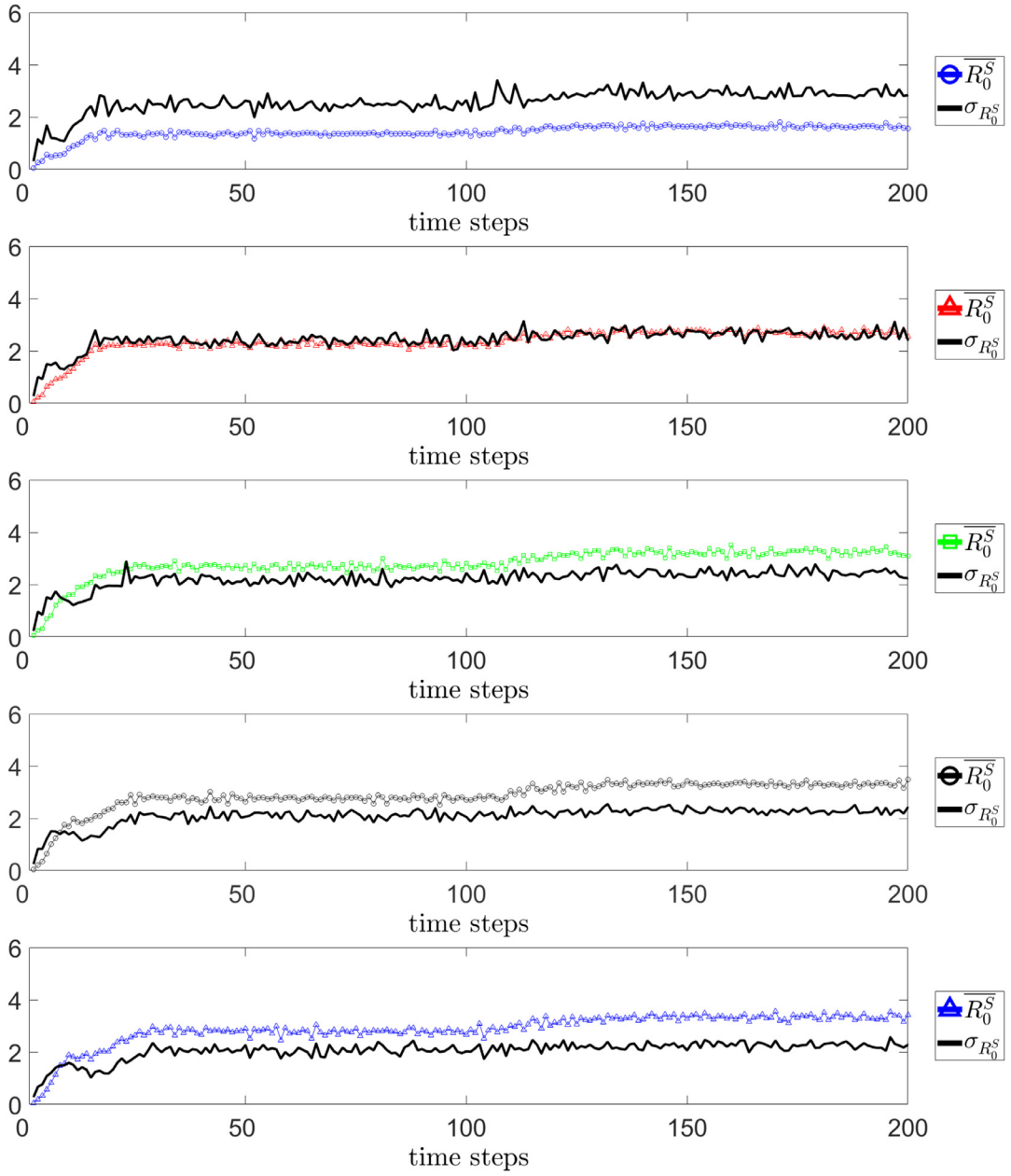

Fig. 8. Time evolution of the average ($\overline{R_0^S}(t)$ - in colours) and standard deviation ($\sigma_{R_0^S}(t)$ - black line) of the spatial basic reproduction number (R_0^S) for distributions β_1, β_4, β_9, β_{16}, and β_{25}, with $P_B = 0.1$.

between the two strains in the infection of susceptible individuals. Naturally, the two serotypes compete for humans $S_{1,2}$, but the second strain can also infect individuals who were infected and recovered from the first serotype (individuals S_2), for instance. Figs. 6 and 8 show the influence of this insertion in the typical R_0 and its spatial version (average R_0^S). The R_0 reduces when the second strain is added into the population, but the average R_0^S increases. It is worth noting that the average R_0^S is an estimation of R_0 for each point of the lattice, and the proposed method considers one infection case multiple times (recall that R_0^S is calculated using states transitions inside a radius for each point of the lattice). Finally, the insertion of a second dengue strain is also essential to consider the antibody-dependent enhancement (ADE) effect, which causes an increase in the probability of death and a reduction in the probability of cure in the case of a second infection of an individual [12,22]. This point increases the importance of the proposed model that assesses all intermediate states in a scenario with the coexistence of two strains, which is consistent with the literature that highlights the low frequency of tertiary and quaternary infections in data from hospital groups [2].

The spatial dynamics of dengue is an important feature for controlling the mosquito population in tropical countries [31]. Not only the breeding sites and vector movement play a role in the spatial distribution of cases, but human movement drives the spread of the virus for distances more significant than the flight range of the vector [5], taking the disease into other regions of the studied map [49]. Moreover, spatial concentrations (clusters) of dengue cases are important to provide intensive interventions to high-risk locations [18].

Therefore, the model presented in this paper can simulate the dengue spreading on real maps to identify the moment of the outbreak, the clusters of the disease and how they evolve

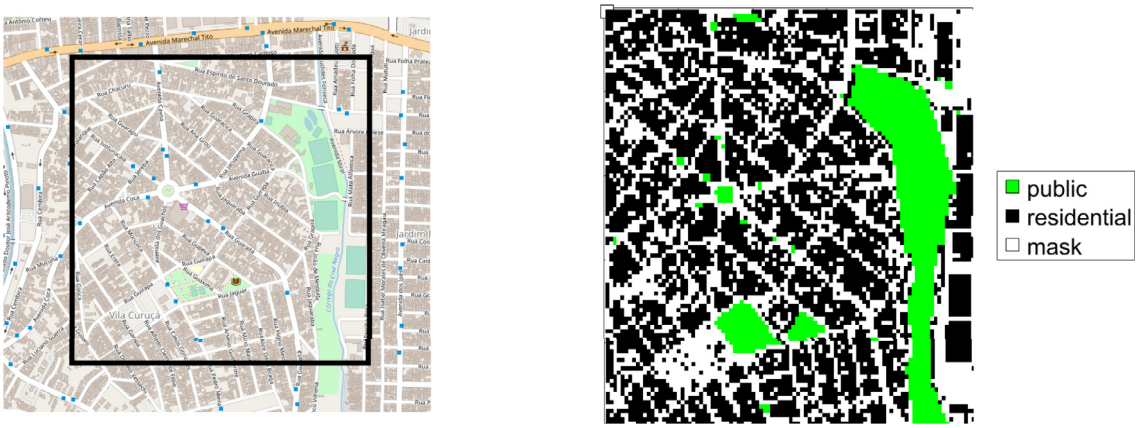

(a) Original map. (b) Map with layers.

Fig. 9. Original map from OpenStreetMap and the final map with layers for public and residential areas, as well as areas with no interest (mask).

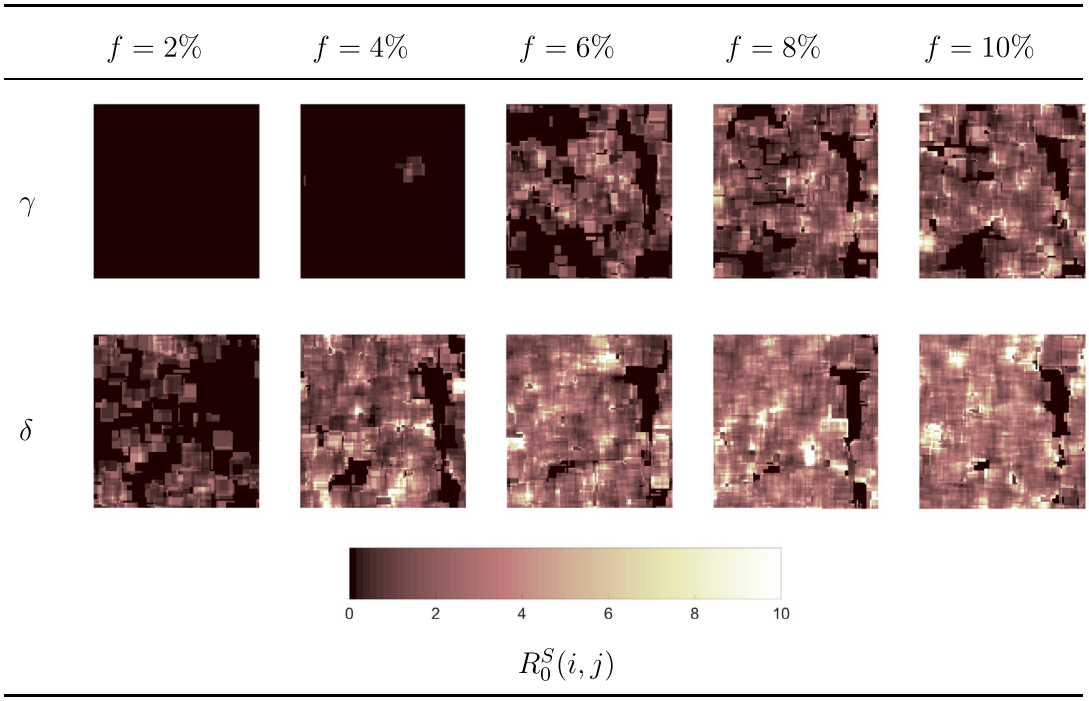

Fig. 10. R_0^S for scenarios δ (breeding cells on public spaces) and γ (breeding cells on residential cells), and five different concentrations (f) at time step $t = 150$, using $P_B = 0.1$. Light colour represents a higher $R_0^S(i,j)$, and the black colour represents $R_0^S(i,j) = 0$.

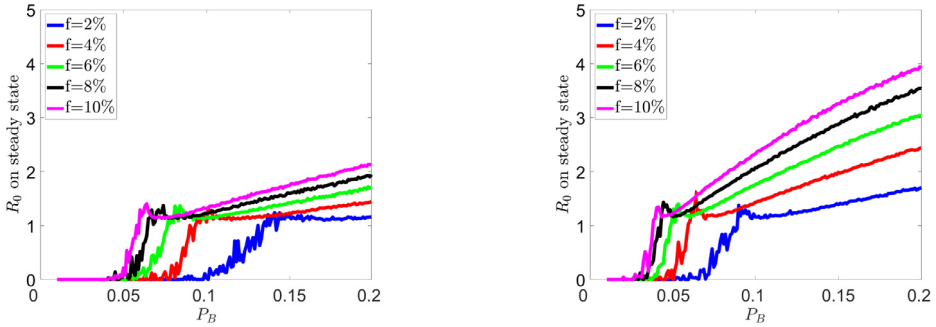

(a) R_0 on steady state for scenario γ. (b) R_0 on steady state for scenario δ.

Fig. 11. R_0 on steady state.

according to human spatial flow. The breeding sites can be either estimated from cluster cases [18,31], sampling female eggs on still water [27,49], or mapping portions of water using Google Earth and GIS (geographic information system) technologies [9]. The United Nations University Institute for Water, Environment and Health developed the Water-Associated Disease Index (WADI) to map existing dengue vulnerability to visualize global regions under threat [19], and map portions could replace the breeding sites with different WADI, which ranges from 0 (low vulnerability) to 1 (highest vulnerability).

The model presented here can be used for future studies. The consideration of more real maps with different human and vector breeding sites distributions and concentrations; adding the *Wolbachia* method to control the dengue propagation on the vector side and simulate the optimal spatial scenarios for releasing infected mosquitoes in a neighbourhood, and; adjusting the model to consider the seasonality of dengue and study the resulting spatial dynamics are some directions of the research.

Statements of ethical approval

Ethics approval was not required for this study.

Funding

PHTS is supported by grants #440025/2020-6, #307194/2019-1 and #402874/2016-1 of Conselho Nacional de Desenvolvimento Científico e Tecnológico (CNPq). FMMP is supported by scholarship grant #88887.505459/2020-0 of Coordenação de Aperfeiçoamento de Pessoal de Nível Superior (CAPES).

Declaration of Competing Interest

The authors declare that they have no known competing financial interests or personal relationships that could have appeared to influence the work reported in this paper.

Acknowledgments

PHTS and FMPP would like to show gratitude to Conselho Nacional de Desenvolvimento Científico e Tecnológico (CNPq), Coordenação de Aperfeiçoamento de Pessoal de Nível Superior (CAPES) and São Paulo Research Foundation (FAPESP) due to the current and past funded projects.

References

[1] M. Aguiar, B. Kooi, N. Stollenwerk, Epidemiology of dengue fever: a model with temporary cross-immunity and possible secondary infection shows bifurcations and chaotic behaviour in wide parameter regions, Math. Model. Nat. Phenom. 3 (4) (2008) 48–70, doi:10.1051/mmnp:2008070.

[2] M. Aguiar, N. Stollenwerk, Mathematical models of dengue fever epidemiology: multi-strain dynamics, immunological aspects associated to disease severity and vaccines, Commun. Biomath. Sci. 1 (1) (2017) 1–12.

[3] M.d.S. Bastos, R.M.P. de Figueiredo, R. Ramasawmy, E. Itapirema, J.B.L. Gimaque, L.O. Santos, L.T.M. Figueiredo, M.P.G. Mourão, Simultaneous circulation of all four dengue serotypes in Manaus, State of Amazonas, Brazil in 2011, Rev. Soc. Bras. Med. Trop. 45 (3) (2012) 393–394, doi:10.1590/s0037-86822012000300022.

[4] J.M.T. Bezerra, S.C.d. Sousa, P.L. Tauil, M. Carneiro, D.S. Barbosa, Entry of dengue virus serotypes and their geographic distribution in Brazilian federative units: a systematic review, Rev. Bras. Epidemiol. 24 (2021) e210020.

[5] P. Bhoomiboonchoo, R.V. Gibbons, A. Huang, I.K. Yoon, D. Buddhari, A. Nisalak, N. Chansatiporn, M. Thipayamongkolgul, S. Kalanarooj, T. Endy, A.L. Rothman, A. Srikiatkhachorn, S. Green, M.P. Mammen, D.A. Cummings, H. Salje, The spatial dynamics of dengue virus in Kamphaeng Phet, Thailand, PLoS Negl. Trop. Dis. 8 (9) (2014) 6–11, doi:10.1371/journal.pntd.0003138.

[6] O.J. Brady, S.I. Hay, The global expansion of dengue: how *Aedes aegypti*mosquitoes enabled the first pandemic arbovirus, Annu. Rev. Entomol. 65 (2020) 191–208.

[7] F. Brauer, C. Castillo-Chavez, A. Mubayi, S. Towers, Some models for epidemics of vector-transmitted diseases, Infect. Dis. Model. 1 (1) (2016) 79–87, doi:10.1016/j.idm.2016.08.001.

[8] P.M. Castanha, M.T. Cordeiro, C.M. Martelli, W.V. Souza, E.T. Marques, C. Braga, Force of infection of dengue serotypes in a population-based study in the northeast of Brazil, Epidemiol. Infect. 141 (5) (2013) 1080–1088, doi:10.1017/S0950268812001367.

[9] A.Y. Chang, M.E. Parrales, J. Jimenez, M.E. Sobieszczyk, S.M. Hammer, D.J. Copenhaver, R.P. Kulkarni, Combining google earth and GIS mapping technologies in a dengue surveillance system for developing countries, Int. J. Health Geogr. 8 (1) (2009) 1–11, doi:10.1186/1476-072X-8-49.

[10] G. Chowell, P. Diaz-Dueñas, J.C. Miller, A. Alcazar-Velazco, J.M. Hyman, P.W. Fenimore, C. Castillo-Chavez, Estimation of the reproduction number of dengue fever from spatial epidemic data, Math. Biosci. 208 (2) (2007) 571–589, doi:10.1016/j.mbs.2006.11.011.

[11] T.E. Colombo, D. Vedovello, A. Mondini, A.F.N. Reis, A.A.F. Cury, F.H. de Oliveira, L.E.A.A. Cruz, R.V.d.M. Bronzoni, M.L. Nogueira, Co-infection of dengue virus by serotypes 1 and 4 in patient from medium sized city from Brazil, Rev. Inst. Med. Trop. Sao Paulo 55 (4) (2013) 275–281, doi:10.1590/S0036-46652013000400009.

[12] W. Dejnirattisai, A. Jumnainsong, N. Onsirisakul, P. Fitton, S. Vasanawathana, W. Limpitikul, C. Puttikhunt, C. Edwards, T. Duangchinda, S. Supasa, K. Chawansuntati, P. Malasit, J. Mongkolsapaya, G. Screaton, Cross-reacting antibodies enhance dengue virus infection in humans, Science 328 (5979) (2010) 745–748, doi:10.1126/science.1185181. http://science.sciencemag.org/content/328/5979/745.full.pdf

[13] P.L. Delamater, E.J. Street, T.F. Leslie, Y.T. Yang, K.H. Jacobsen, Complexity of the basic reproduction number (R0), Emerg. Infect. Dis. 25 (1) (2019) 1–4, doi:10.3201/eid2501.171901.

[14] O. Diekmann, J. Heesterbeek, M.G. Roberts, The construction of next-generation matrices for compartmental epidemic models, J. R. Soc. Interface 7 (2010) 873–885.

[15] O. Diekmann, J.A. Heesterbeek, J.A. Metz, On the definition and the computation of the basic reproduction ratio R0 in models for infectious diseases in heterogeneous populations, J. Math. Biol. 28 (4) (1990) 365–382, doi:10.1007/BF00178324.

[16] J. Fang, X. Lai, F.B. Wang, Spatial dynamics of a dengue transmission model in time-space periodic environment, J. Differ. Equ. 269 (8) (2020) 149–175, doi:10.1016/j.jde.2020.04.034.

[17] R.M. de Figueiredo, F.G. Naveca, C.M. Oliveira, M. de Souza Bastos Bastos, M.P.G. Mourão, S. de S Viana, M. do N Melo, E.F. Itapirema, C.J. Saatkamp, I.P. Farias, Co-infection of dengue virus by serotypes 3 and 4 in patients from Amazonas, Brazil, Rev. Inst. Med. Trop. Sao Paulo 53 (6) (2011) 321–323, doi:10.1590/S0036-46652011000600004.

[18] L.P. Freitas, O.G. Cruz, R. Lowe, M. S Carvalho, Space-time dynamics of a triple epidemic: dengue, Chikungunya and Zika clusters in the city of rio de janeiro, Proc. R. Soc. B 286 (1912) (2019) 20191867, doi:10.1098/rspb.2019.1867.

[19] L. Fullerton, S. Dickin, C.J. Schuster-Wallace, Mapping Global Vulnerability to Dengue using the Water Associated Disease Index Waste to Wealth View project, United Nations University, 2012. https://www.researchgate.net/publication/273439367

[20] S.M. Garba, A.B. Gumel, M.R. Abu Bakar, Backward bifurcations in dengue transmission dynamics, Math. Biosci. 215 (1) (2008) 11–25, doi:10.1016/j.mbs.2008.05.002.

[21] R. Gautam, S. Mishra, A. Milhotra, R. Nagpal, M. Mohan, A. Singhal, P. Kumari, Challenges with mosquito-borne viral diseases: outbreak of the monsters, Curr. Top. Med. Chem. 17 (19) (2017) 2199–2214.

[22] M.G. Guzman, S. Vazquez, The complexity of antibody-dependent enhancement of dengue virus infection, Viruses 2 (12) (2010) 2649–2662, doi:10.3390/v2122649.

[23] S.B. Halstead, Dengue, Tropical Medicine: Science and Practice, Imperial College Press, London, 2008.

[24] H. Harapan, A. Michie, R.T. Sasmono, A. Imrie, Dengue: a minireview, Viruses 12 (8) (2020) 829.

[25] N.A. Hartemink, B.V. Purse, R. Meiswinkel, H.E. Brown, A. de Koeijer, A.R. Elbers, G.J. Boender, D.J. Rogers, J.A. Heesterbeek, Mapping the basic reproduction number (R0) for vector-borne diseases: a case study on bluetongue virus, Epidemics 1 (2009) 153–161, doi:10.1016/j.epidem.2009.05.004.

[26] H. Heesterbeek, R.M. Anderson, V. Andreasen, S. Bansal, D. De Angelis, C. Dye, K.T. Eames, W.J. Edmunds, S.D. Frost, S. Funk, et al., Modeling infectious disease dynamics in the complex landscape of global health, Science 347 (6227) (2015).

[27] N.A. Honório, W. Da Costa Silva, P.J. Leite, J.M. Gonçalves, L.P. Lounibos, R. Lourenço-de Oliveira, Dispersal of *Aedes aegypti* and *Aedes albopictus*(diptera: culicidae) in an urban endemic dengue area in the State of Rio de Janeiro, Brazil, Mem. Inst. Oswaldo Cruz 98 (2) (2003) 191–198, doi:10.1590/S0074-02762003000200005.

[28] Jafaruddin, S.W. Indratno, N. Nuraini, A.K. Supriatna, E. Soewono, Estimation of the basic reproductive ratio for dengue fever at the take-off period of dengue infection, Comput. Math. Methods Med. 2015 (2015), doi:10.1155/2015/206131.

[29] B.W. Kooi, M. Aguiar, N. Stollenwerk, Analysis of an asymmetric two-strain dengue model, Math. Biosci. 248 (2014) 128–139, doi:10.1016/j.mbs.2013.12.009.

[30] M. Kretzschmar, Measurement and modeling: Infectious disease modeling, Reference Module in Biomedical Sciences, Elsevier, 2016, doi:10.1016/B978-0-12-801238-3.98837-8. https://www.sciencedirect.com/science/article/pii/B9780128012383988378

[31] R.M. Lana, T.G.S.C. Carneiro, N.A. Honrio, C.T. Codeço, Mapping the basic reproduction number (R0) for vector-borne diseases: a case study on bluetongue

virus, J. Inf. Data Manag. 2 (2) (2011) 211–220, doi:10.1016/j.epidem.2009.05.004.
[32] J.T. Lim, B.S.L. Dickens, L.Z.X. Chew, E.L.W. Choo, J.R. Koo, J. Aik, L.C. Ng, A.R. Cook, Impact of SARS-CoV-2 interventions on dengue transmission, PLoS Negl. Trop. Dis. 14 (10) (2020) e0008719.
[33] M.J.W. Lindström, et al., Understanding the spread and eradication of novel zoonotic diseases through the study of a compartmental epidemiological model(2020).
[34] Y. Liu, K. Lillepold, J.C. Semenza, Y. Tozan, M.B. Quam, J. Rocklöv, Reviewing estimates of the basic reproduction number for dengue, Zika and Chikungunya across global climate zones, Environ. Res. 182 (January) (2020) 109114, doi:10.1016/j.envres.2020.109114.
[35] T.A. McLennan-Smith, G.N. Mercer, Complex behaviour in a dengue model with a seasonally varying vector population, Math. Biosci. 248 (2014) 22–30, doi:10.1016/j.mbs.2013.11.003.
[36] P. Mendes Luz, C. Torres Codeço, E. Massad, C.J. Struchiner, Uncertainties regarding dengue modeling in Rio de Janeiro, Brazil, Mem. Inst. Oswaldo Cruz 98 (7) (2003) 871–878, doi:10.1590/s0074-02762003000700002.
[37] L. Monteiro, D. Gandini, P. Schimit, The influence of immune individuals in disease spread evaluated by cellular automaton and genetic algorithm, Comput. Methods. Prog. Biomed. 196 (2020) 105707.
[38] E.A. Mordecai, J.M. Caldwell, M.K. Grossman, C.A. Lippi, L.R. Johnson, M. Neira, J.R. Rohr, S.J. Ryan, V. Savage, M.S. Shocket, et al., Thermal biology of mosquito-borne disease, Ecol. Lett. 22 (10) (2019) 1690–1708.
[39] T.C. Ng, T.H. Wen, Spatially adjusted time-varying reproductive numbers: understanding the geographical expansion of urban dengue outbreaks, Sci. Rep. 9 (1) (2019) 1–12, doi:10.1038/s41598-019-55574-0.
[40] M. Nicoletti, Three scenarios in insect-borne diseases, in: Insect-Borne Diseases in the 21st Century, 2020, p. 99.
[41] J.F. Oliveira, M.S. Rodrigues, L.M. Skalinski, A.E. Santos, L.C. Costa, L.L. Cardim, E.S. Paixão, M.d.C.N. Costa, W.K. Oliveira, M.L. Barreto, et al., Interdependence between confirmed and discarded cases of dengue, Chikungunya and Zika viruses in Brazil: a multivariate time-series analysis, PLoS One 15 (2) (2020) e0228347.
[42] OpenStreetMap contributors, Planet dump retrieved from https://planet.osm.org, 2017, (https://www.openstreetmap.org).
[43] K.M. OReilly, E. Hendrickx, D.D. Kharisma, N.N. Wilastonegoro, L.B. Carrington, I.R. Elyazar, A.J. Kucharski, R. Lowe, S. Flasche, D.M. Pigott, et al., Estimating the burden of dengue and the impact of release of wMel *Wolbachia*-infected mosquitoes in Indonesia: a modelling study, BMC Med. 17 (1) (2019) 1–14.
[44] W.H. Palmer, F.S. Varghese, R.P. Van Rij, Natural variation in resistance to virus infection in dipteran insects, Viruses 10 (3) (2018) 118.
[45] T. Pang, T.K. Mak, D.J. Gubler, Prevention and control of dengue the light at the end of the tunnel, Lancet Infect. Dis. 17 (3) (2017) e79–e87.
[46] P.E. Parham, J. Waldock, G.K. Christophides, D. Hemming, F. Agusto, K.J. Evans, N. Fefferman, H. Gaff, A. Gumel, S. LaDeau, et al., Climate, environmental and socio-economic change: weighing up the balance in vector-borne disease transmission, Philos. Trans. R. Soc. B 370 (1665) (2015) 20130551.
[47] F.M.M. Pereira, P.H.T. Schimit, Dengue fever spreading based on probabilistic cellular automata with two lattices, Phys. A 499 (2018) 75–87, doi:10.1016/j.physa.2018.01.029.
[48] QGIS Development Team, QGIS Geographic Information System, Open Source Geospatial Foundation, 2009. http://qgis.osgeo.org
[49] L.N. Regis, R.V. Acioli, J.C. Silveira, M.A.V. de Melo-Santos, M.C.S. da Cunha, F. Souza, C.A.V. Batista, R.M.R. Barbosa, C.M.F. de Oliveira, C.F.J. Ayres, A.M.V. Monteiro, W.V. Souza, Characterization of the spatial and temporal dynamics of the dengue vector population established in urban areas of Fernando de Noronha, a Brazilian oceanic island, Acta Trop. 137 (2014) 80–87, doi:10.1016/j.actatropica.2014.04.010.
[50] B.B. Salgado, F.C. de Jesus Maués, R.L. Pereira, J.O. Chiang, M.N. de Oliveira Freitas, M.S. Ferreira, L.C. Martins, P.F. da Costa Vasconcelos, C. Ganoza, P. Lalwani, Prevalence of arbovirus antibodies in young healthy adult population in Brazil (2021).
[51] P. Schimit, A model based on cellular automata to estimate the social isolation impact on COVID-19 spreading in Brazil, Comput. Methods Prog. Biomed. 200 (2021) 105832.
[52] P.H.T. Schimit, L.H.A. Monteiro, On the basic reproduction number and the topological properties of the contact network: an epidemiological study in mainly locally connected cellular automata, Ecol. Model. 220 (2009) 1034–1042.
[53] W.R. Shaw, F. Catteruccia, Vector biology meets disease control: using basic research to fight vector-borne diseases, Nat. Microbiol. 4 (1) (2019) 20–34.
[54] M.F.F. Sobral, A.I.G. Da Penha Sobral, Cases of dengue and urban waste collection: a study in the city of Recife, Ciencia Saude Coletiva 24 (3) (2019) 1075–1082, doi:10.1590/1413-81232018243.10702017.
[55] P.M. São Paulo, Dengue - srie histrica de 2007 a 2021 - dve - covisa, 2021, (https://www.prefeitura.sp.gov.br/cidade/secretarias/saude/vigilancia_em_saude/index.php?p=245603).
[56] P. Van Den Driessche, J. Watmough, Reproduction numbers and subthreshold endemic equilibria for compartmental models of disease transmission, Math. Biosci. 180 (1–2) (2002) 29–48, doi:10.1016/S0025-5564(02)00108-6.
[57] S. Vanwambeke, P. Schimit, Tick bite risk resulting from spatially heterogeneous hazard, exposure and coping capacity, Ecol. Complex. 48 (2021) 100967, doi:10.1016/j.ecocom.2021.100967. https://linkinghub.elsevier.com/retrieve/pii/S1476945X2100060X
[58] S.O. Vanwambeke, S.N. Bennett, D.D. Kapan, Spatially disaggregated disease transmission risk: land cover, land use and risk of dengue transmission on the island of Oahu, Trop. Med. Int. Health 16 (2) (2011) 174–185.
[59] C.J. Villabona-Arenas, J.L. de Oliveira, C.S. de Capra, K. Balarini, M. Loureiro, C.R.T.P. Fonseca, S.D. Passos, P.M.A. de Zanotto, Detection of four dengue serotypes suggests rise in hyperendemicity in urban centers of Brazil, PLoS Negl. Trop. Dis. 8 (2) (2014) 3–5, doi:10.1371/journal.pntd.0002620.
[60] H.M. Yang, The basic reproduction number obtained from jacobian and next generation matrices a case study of dengue transmission modelling, BioSystems 126 (2014) 52–75, doi:10.1016/j.biosystems.2014.10.002.
[61] H.M. Yang, C.P. Ferreira, Assessing the effects of vector control on dengue transmission, Appl. Math. Comput. 198 (1) (2008) 401–413, doi:10.1016/j.amc.2007.08.046.
[62] Y. Yue, X. Liu, D. Ren, H. Wu, Q. Liu, Spatial dynamics of dengue fever in mainland China, 2019, Int. J. Environ. Res. Public Health 18 (6) (2021) 1–12, doi:10.3390/ijerph18062855.
[63] L. Zhao, Z.C. Wang, S. Ruan, Dynamics of a time-periodic two-strain sis epidemic model with diffusion and latent period, Nonlinear Anal. 51 (2020), doi:10.1016/j.nonrwa.2019.102966.